YZrO2-Ni Cermet Processing by High Energy Milling

Thomaz A. Guisard Restivo[1,a], Sonia R. H. Mello Castanho[2,b]

[1,2]Centro de Ciências e Tecnologia de Materiais – CCTM – IPEN

Av. Lineu Prestes 2242 – Cidade Univerrsitária – 05508000 – São Pualo – SP BRASIL

[a]guisard@dglnet.com.br, [b]srmello@ipen.br

Keywords: SOFC, anode, sintering, cermet, high energy milling, mechanical alloying

Abstract

A new method for SOFC fuel cell anode preparation is proposed where the main difference lies over cermet powder processing by high energy milling. Yttria stabilized zirconia powder and metallic nickel undergo co-milling in a vibratory device employing zirconia bead media. Dispersed and homogeneous powders are therefore obtained. The material is pressed uniaxialy and sintered at 1350°C for 0,5 h in air and under argon and hydrogen. In the former case, partial nickel oxidation occurs before sintering leading to small shrinkage down to 2% and porosity about 38%. Linear shrinkages from 5 to 7% after sintering in both inert and reduced atmospheres were observed not demanding pore-former additives. Conventional YSZ, Ni and NiO powder mixtures were prepared for comparison purpose. The high energy milling process is able to reduce the starting sintering temperature by 130° C besides a higher densification compared to the simple mixtures YSZ+Ni. The excessive sintering and particle coalescence is absent in high energy milled material, where the metal is well dispersed and the microstructure is highly homogenous. The high energy milling process is a promising route to prepare with excellent performance anode materials for SOFC cells.

Introduction

Solid oxide fuel cell (SOFC) has been considered to participate in energetic generation systems wide world due to its high conversion efficiency and energy output besides lower polluant release. The inclusion of SOFC devices in Brazilian energetic matrix is attractive since the country has been developed extensive production structure based on ethanol and biogas fuels since 30 years ago. In this scenery, it is fundamental to overcome the difficulties related to direct reforming of available fuels from organic sources. SOFC devices are built by associating 4 components [1, 2]: fuel anode, air cathode, solid electrolyte and interconnect. The anode concentrates several functions like fuel oxidation, related to the electrocatalytic activity, electronic conductivity, O^{2-} ion transport originating from the YSZ electrolyte and direct reforming of hydrocarbon or alcohol fuels in such cases. The last capability leads to hydrogen rich gas which undergoes further electrochemical reactions. The most considered anode material for SOFC is YSZ-Ni cermet, which holds all the desired characteristics together with its stability and chemical and expansion compatibility with the electrolyte [3].

The conventional preparation route for YSZ-Ni anodes consists on mixing YSZ and NiO oxides followed by sintering in oxidant atmosphere and a further reduction step at 900-1000°C or in situ by the fuel during the SOFC operation [2, 4, 5]. The shrinkage produced by the reduction of NiO to Ni is quite small. A common practice is to include pore-forming additives, like graphite, in order to reach a suitable porosity range for gas flow (40-60%) [4].

Mechanical alloying (MA) is a high energy milling process wich has been employed to obtain amorphous materials, supersaturated solid solution materials, nanomaterials and cermets [6-10]. MA has been used for obtain YSZ-Ni cermets for high temperature electrolysis [11] as well as for SOFC anode material preparation [12]. This work aims to contribute by introducing a new route for anode preparation to obtain better performance in SOFC devices. The anode cermet $YZrO_2$-Ni (YSZ-Ni) material is prepared by high energy milling of YSZ and metallic Ni powders and sintering. The objective is to improve the process and the microstructure to maximise 3-point

boundary sites concentration by particle refining and optimizing the components dispersion. Therefore high electrocatalytic activity is envisioned besides good electric percolation as well as gas reagents and products diffusion through the pores. The method is also expected to reduce the sintering temperature and simplify the process steps. Process parameters evaluation, simulation by dilatometry and characterization of powders and pellets are shown.

Experimental

Starting powders consist on YSZ (8mols%Y_2O_3, Tosoh Corp.) and metallic Ni (CIRQ Cromato, 400 mesh, 99,6wt% purity). The BET and average particle size values for the former were 13m^2/g and 0,3μm and for the last 0,3m^2/g and 29,3μm. For comparison, NiO (PA-ACS, high purity) was employed to prepare conventional YSZ-NiO powder mixtures. The obtained samples were characterised by BET, laser granulometer (CILAS 1064) and X-ray diffraction (Rigaku). Two vibratory mills were employed: SPEX 8000M (29 Hz) and a variable speed vibratory home-made mill rated at 10 Hz. YTZ or hard steel milling spheres with ball to powder mass ratio at 10:1 were used in all experiments. UHMW polyethylene vials tide sealed by means of an o'ring were used as the vibratory container. Each sample preparation used 10 g total powder mass where the mixture composition was 50wt%YSZ – 50wt%Ni, chosen to meet the normal average content at a SOFC anode. The process parameters varied included the time of milling, atmosphere into the vial (glove-box charging) and rotation speed. Table 1 lists the sample obtained during the study.

sample	Atmosphere	Milling time[h]	Milling media	Rotation [Hz]
1A1H	Air	1	YTZ	29
2A1H	Air	1	Steel	29
3ASMIX*	Air	3	Alumina	5
4ASMIX**	Air	3	Alumina	5
5A2H	Air	2	YTZ	29
6A2H	Argon	2	YTZ	29
8B4H	Air	4	YTZ	10
8C8H	Air	8	YTZ	10
10A16H	Air	16	YTZ	10
12A4H	Argon	4	YTZ	29
12A8H	Argon	8	YTZ	29

* simple mixing slurry 50w%YSZ – 50w%Ni

** simple mixing slurry 41,5w%YSZ – 58,5w% NiO

Table 1. Powder samples prepared by high energy milling (MA).

Some sample mixed powders were prepared for comparison by 3wt% PVA alcohol slurry conventional ball milling method, followed by drying and deagglomeration. The powder samples were screened through a 200μm sieve and pressed uniaxially at 200MPa to conform green pellets 7mm diameter. The pellets were sintered in both air and argon flowing gases in a muffle furnace and also in a vertical dilatometer (Setaram Labsys TMA 1400°C). The heating rate was 10°C/min up to 1300 and 1350°C, maintained for 0,5 and 1 hours at the isotherm. The TMA load for all experiments was set as 2g in order to cause no influence on sintering profiles. One sample was sintered at Setaram's Demonstration Lab in Lyon at another TMA model (Setsys TMA 1750°C) under pure hydrogen. The sintered pellets were polished and observed at a SEM (Philips XL30). The powder morphology was also observed in vacuum impregnated green pellets samples.

Results and Discussion

The high energy milled powder particle sizes reach an equilibrium mean value of about 5-6μm for increasing milling times in all conditions, even comparing the high powered milling device (29Hz) with the slower one (10Hz). Sample mixtures BET analysis has shown a surface area

development as a function of time and rotation speed in the range 7,6 - 12,6 m^2/g. Fig.1 shows the refining tendency for the two rotation and atmosphere conditions. The particle refining speed is greater for high rotation milling once 2 hours process is enough to attain 6μm size. From the data and powder characteristic noted after MA, it is suggested the small oxidation in air milled sample can work as process controller avoiding excessive Ni cold welding, leading to smaller particle sizes in less time. Mass losses of the powder samples 5A2H and 6A2H were measured by thermogravimetric analysis up to 950°C at 10°C/min in N_2-4%H_2 as –1,85% (air milled) and –2,98% (argon milled), related to the Ni oxide reduced. Apparently the air milled powder underwent passivation inside the vial during the process increasing its stability to handling operations.

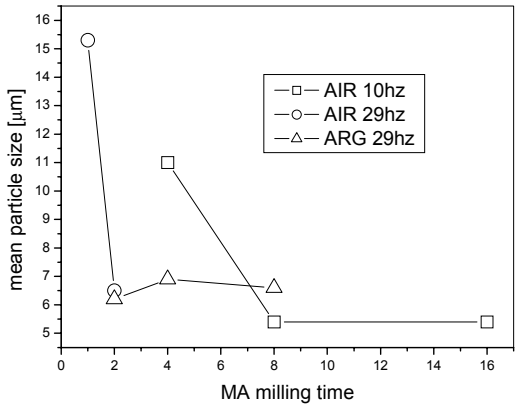

Fig.1. Mean particle sizes evolution after MA as a function of time and atmosphere.

The MA powders were analysed by X-ray diffraction to identify the phases and evaluate the amount of refining, deformation and alloying caused by the process. One can see in Fig.2(a) for sample 6A2H the only peaks detected correspond to YSZ and Ni starting materials whereas exhibiting strong peak broadening, specially at Ni lines. The effect is due particle refining and increasing defects concentration that develops subgrains in the metal structure. The particle refining itself can explain the broadening at YSZ peaks. Fig.2(b) compiles some X-ray profiles for powder samples in different conditions. One Ni peak is hardly observed in sample 12A8H (2θ = 51,925° measured; expected intensity 42%) or at least superimposed on the preceding YSZ peak, suggesting the metal approaches the amorphous condition. Displacement of Ni and YSZ X-ray peaks are emphasised in Fig.2(c). The Ni peaks have been strongly shifted to smaller angles for sample 12A8H, whereas the YSZ peaks are slightly shifted to higher ones. The results indicate C atom has diffused to form a supersaturated solid solution in Ni lattice while NiO oxide can be solved in YSZ, in agreement with the refs.[12] and [13]. The Ni peak shifting is more important for the highest energetic processed samples. Moreover Ni_3C phase (JCPDS 77-0194) has been only detected in powder 12A8H. The C saturated Ni and the carbide are formed probably by contamination from the polyethylene vial once most part of the powder remained encrusted.

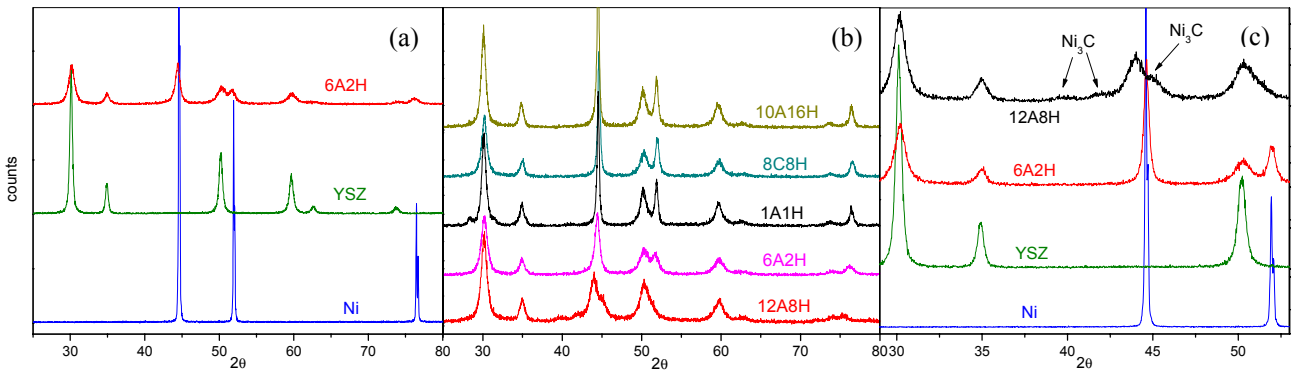

Fig.2 X-ray profiles: (a) YSZ and Ni starting materials and one MA milled powder; (b) main powder samples; (c) peak shift detail showing phase formation.

Sintering of sample pellets at a dilatometer/TMA is shown in Fig.3. For air sintering (Fig.3(a)), the Ni powder in the cermet undergoes oxidation before shrinkage with corresponding expansion. Dilatometric curves for the MA processed powders show higher sintering start temperatures compared to YSZ and YSZ-NiO. The sintering starts when the expansion caused by the oxidation is surpassed by the shrinkage. Among the MA powders, the higher the energy of milling the lower the sintering start temperature: for instance, sample 1A1H shows a reduction on sintering start temperature of 130°C compared to simple mixed 3ASMIX sample (990 against 1120°C). However, powder 6A2H has a second oxidation step which delays shrinkage.

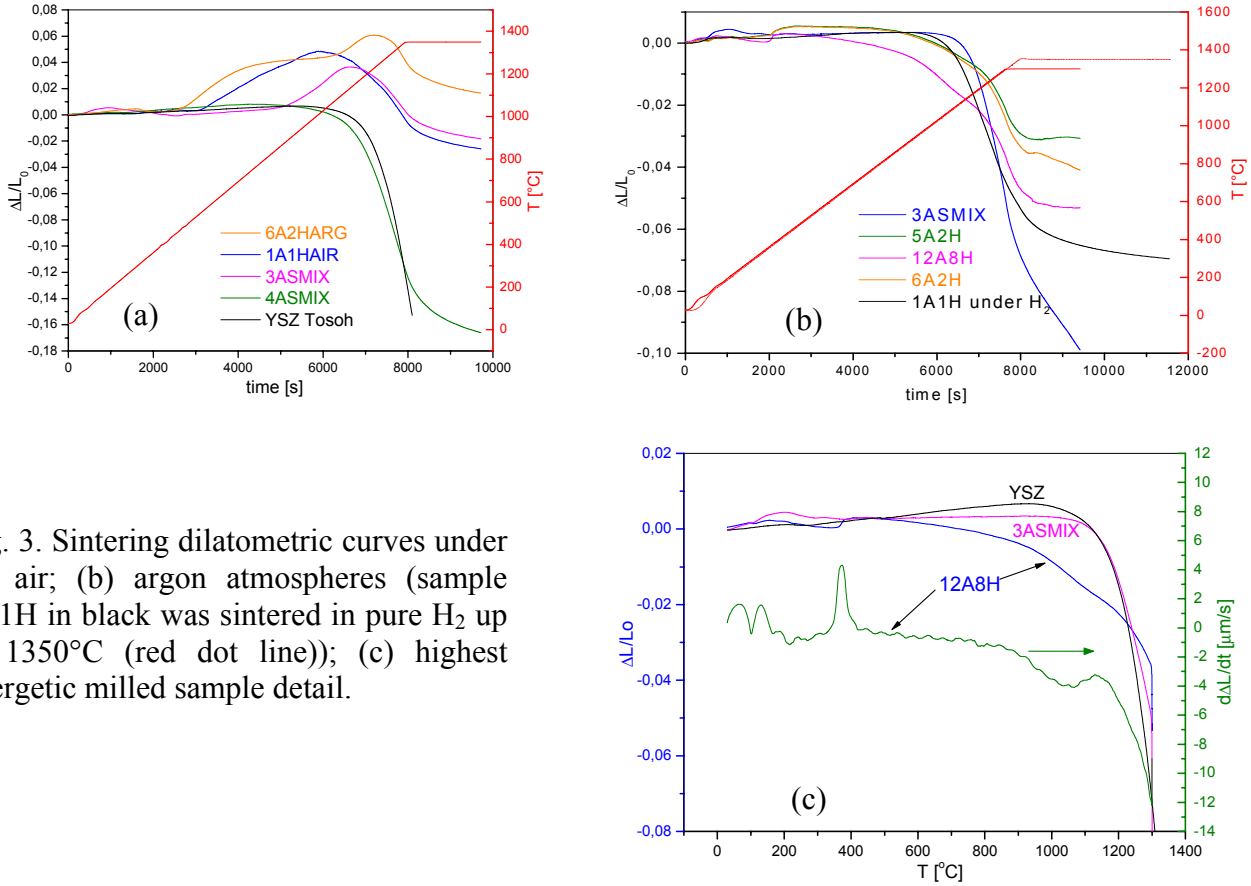

Fig. 3. Sintering dilatometric curves under (a) air; (b) argon atmospheres (sample 1A1H in black was sintered in pure H_2 up to 1350°C (red dot line)); (c) highest energetic milled sample detail.

In argon sintering atmosphere (Fig.3(b)) the behaviour is totally different. The MA milled cermet powders start sintering at lower temperatures from 460°C up to 800°C having an inverse dependence of the milling time. These temperatures are far bellow than the simple mixing Ni-YSZ and YSZ samples (966 and 1021°C). Also, the MA milled powders attain higher densification as the milling energy delivered is higher. Fig.3(c) evaluates the sintering process for the highest energetic generated powder by MA. One can see the sintering process has 2 steps related to earlier Ni sintering and later to the YSZ one. The pellet starts sintering slowly at 195°C afterward showing an expansion and definitively resumes sintering at 460°C. Ceramic fine particle dispersion is said to inhibit Ni sintering [14] while very thin and deformed metal particles have been found to start sintering at temperatures as low as 200°C or less [15, 16]. The balance among these two influences leads to the actual sintering behaviour. Since liquid phase sintering takes place for this sample, it implies an eutectic alloy must be formed between Ni (Zr) and C. It has been reported based on DSC measurements [13] the C supersaturated Ni decomposes into Ni and Ni_3C at 318°C and afterwards into Ni and C at 460°C. Actually, there are some candidates to eutectic alloys at the respective ternary and pseudobinary phase diagrams. Careful examination of sintering curves demonstrates the 2-step sintering is assigned for the other MA samples. In previous work [17,18], the authors have demonstrated the ability of high active carbon to react with stable oxides like Al_2O_3 and ZrO_2, regarding a solvent metallic bath is present.

Fig.4 shows SEM images displaying MA powders morphologies. Powder sample 6A2H (Fig.4(a)) features metallic Ni deformed plates partially recovered by smaller YSZ particles. The 3 remaining images were obtained from polished vacuum impregnated green pellets. It can be seen the particles have a MA typical lamellar structure that has disappeared at sample 12A8H highest energetic milled. EDS punctual measurements detected both Zr and Ni into the main particles, that are unresolved by SEM magnification level. Few YSZ particles are hardly seen as small bright spheres, meaning the most part is intimated mixed with Ni. There is a particle coarsening tendency as the MA time increases.

(a) 6A2H 29hz MA argon (SE)

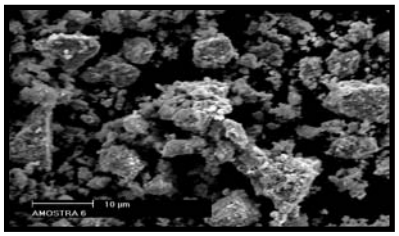

(b) 8C8H 10hz MA in air (BSE)

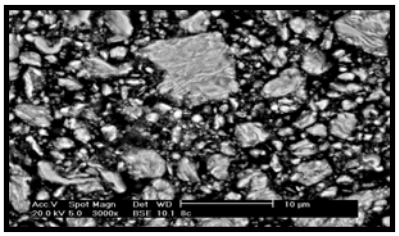

(c) 12A4H 29hz MA argon (BSE)

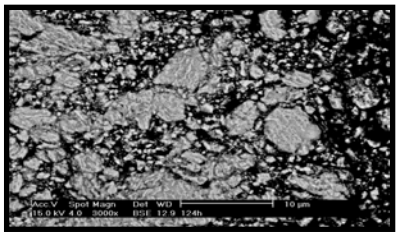

(d) 12A8H 29hz MA argon (BSE)

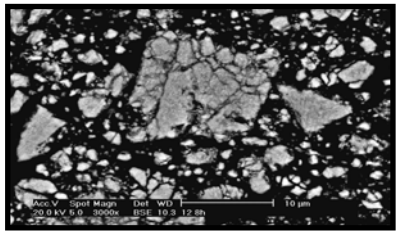

Fig.4. Powder morphologies after MA in various milling conditions.

Sintered pellet SEM microstructures are shown in Fig.5 for simple mixed, 6A2H and 12A8H materials. It is easily recognised the YSZ original agglomerates at 3ASMIX sample while unresolved for the MA powder pellets. EDS measurements in different fields is unable to identify the starting components, indicating the YSZ constituent may be finely dispersed. The occurrence of liquid phase sintered can be inferred since the grains are coarsen and filled by a darker field. The internal structure is progressively refined as the MA time is increased. One small metal droplet recovered from the 12A8H pellet after sintering has a typical hypoeutectic alloy microstructure consisting of primary Ni grains surrounded by lamellar eutectic constituent.

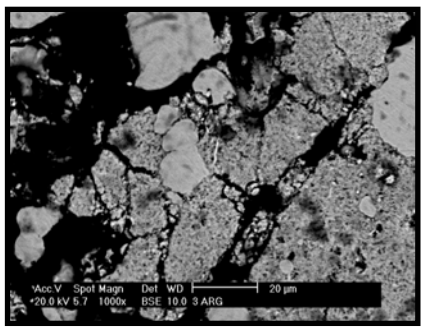

(a) 3ASMIX

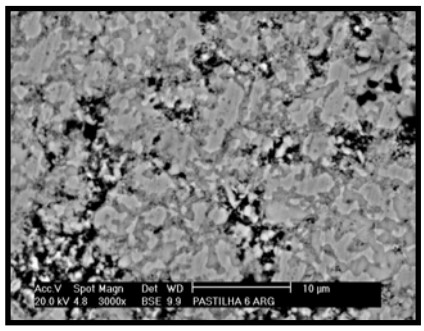

(b) 6A2H MA

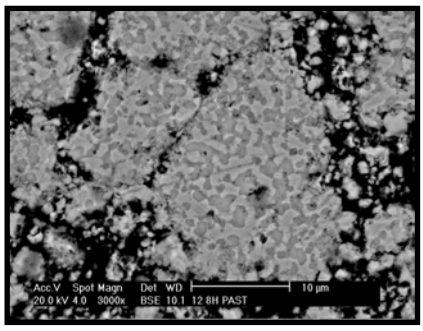

(c) 12A8H

Fig. 5. Sintered pellets microstructure SEM images (BSE)

Some pellet samples of different conditions were sintered in a tubular furnace under argon atmosphere at 1300°C for 1 hour in order to evaluate final geometric densities (Table 2). The sintered pellet densities fall in the expected range for SOFC anodes (60-80%TD). The MA processed powder pellets are more porous as the milling energy is higher.

sample	Milling time/ atm / hz	Green TD (%)	Sintered TD (%)
12A8H	8 / argon / 29	47,96	68,59
10A16H	16 / air / 10	55,04	68,77
8D16H	16 / air / 10	55,20	65,89
8C8H	8 / air / 10	56,28	69,38
8B4H	4 / air / 10	57,32	71,24
8A2H	2 / air / 10	58,98	75,07
6A2H	2 / argon / 29	55,88	65,36
5A2H	2 / air / 29	54,93	65,28
3ASMIX	---	56,78	74,09
1A1H	1 / air / 29	50,78	67,22
Pure Ni	---	68,23	76,28

Table 2. Geometric densities of sintered pellets (TD assumed as 7,239g/cm^3).

Conclusions

Mechanical alloying is a promised processing route for preparation SOFC anodes. The association of Ni and YSZ by co-milling the powders can lead to well dispersed powder mixtures and homogeneous sintered pellets, maintaining the desired porosity for gas diffusion. The method dispenses pore former additives and can be carried out in one sole step. Ceramic processing parameters like green density and sintering temperature can be easily adjusted for the desired microstructure and porosity. The milling parameters can also be controlled in order to obtain suitable materials. The higher the milling energy delivered to a powder, the lower the sintered density. Sintering start temperatures are strongly lowered as the MA time and energy increase. Shrinkages were assigned at temperatures as low as 195°C and 460°C, which is far lower than simple mixing YSZ-Ni powder (966°C). MA processed powders at longer times and energies can lead to supersaturated Ni-C solid solutions causing liquid phase sintering to occur. However, some actions can be made to avoid these effects like vial material selection, cooling and control of milling time and energy and also by admixing process control, dispersing and lubricant additives.

Acknowledge. The authors acknowledge Mr. Luc Benoist from Setaram Lab Lyon for carrying out some dilatometries, FAPESP/SP and CNPq both for financial support.

References

[1] A. Atkinson, et al.: Nature Materials 3, 1, (2004).
[2] N.Q. Minh: J. Am. Ceram. Soc. 76 [3], 563-88 (1993).
[3] C. Keegan, J.S. Cooper: Journal of Power Sources 140 (2), 280-296 (2005).
[4] J. Sankar, Z. Xu, S. Yarmolenko: FY 2005 Progress Report for Heavy Vehicle Propulsion Materials, 4D. Processing and Characterization of Structural and Functional Materials for Heavy-Vehicle Applications, 89-97, (may 2006).
[5] C. Sun, U. J. Stimming: Power Sources (2007), oi:10.1016/j.jpowsour.2007.06.086
[6] C.C. Koch: Metallurgical Transactions A, 19A, 2867-74 (dec1988).
[7] A.W. Weeber, H. Bakker: Physica B 153, 93-135 (1988).
[8] K. Morsi, S. Shinde, E.A. Olevsky: Mat. Sci. and Eng. A 426, 283–288 (2006).
[9] Chul-Jin Choi, J. Mat. Proc. Tech. 104, 127 (2000).
[10] J. L. Guichard, 0. Tillement and A. Mocellin: J. Eur. Ceram. Soc. 18, 1143- 1152 (1998).
[11] H.S. Hong et al.: Journal of Power Sources 149, 84–89 (2005).
[12] R. Wilkenhoener: Journal of Materials Science 34, 257– 265 (1999).
[13] T. Tanaka, K.N. Ishihara, P.H. Shingu: Metallurgical Transactions A, 23A, 2431 (1992).
[14] M. F. Ashby et al.: Progress In Materials Science Vol. 25, p. 1-34 (1980).
[15] B.B. Panigrahi: Materials Science and Engineering A, 460-461, 7-13 (2007).
[16] Y.H. Zhou, M. Harmelin, J. Bigot: Materials Science and Engineering A113, 775-79 (1991).
[17] T.A.G. Restivo, J.D.T. Capocchi: J. Nuclear Materials 334, 189-194 (2004).
[18] T.A.G. Restivo: PhD Thesis, Escola Politécnica USP, 106p. (2003).